J Supercond Nov Magn (2013) 26:879–884
DOI 10.1007/s10948-012-1976-4

ORIGINAL PAPER

The Effect of Silver Inclusion on Superconducting Properties of $YBa_2Cu_3O_y$ Prepared Using Planetary Ball Milling

A. Hamrita · F. Ben Azzouz · W. Dachraoui · M. Ben Salem

Received: 2 November 2012 / Accepted: 1 December 2012 / Published online: 25 January 2013

Abstract The effect of Ag inclusion on the structure microstructure and the critical current density of the $YBa_2Cu_3O_{7-\delta}$ sample prepared using the planetary ball milling process has been investigated. $YBa_2Cu_3O_{7-\delta}$ ceramics have been synthesized in air by a solid state reaction method from an oxide precursor powder, which was prepared from the starting powders of Y_2O_3, Ba_2CO_3, and CuO via a one-step annealing process in air at 950 °C. After planetary ball milling for 4 h of the oxide precursor powders, it was mixed with an $AgNO_3$ solution, and then was dried and uniaxially pressed, and subsequently annealed at 950 °C in air. Phase analysis by X-ray diffraction (XRD), granular structure examination by scanning electron microscopy (SEM), microstructure investigation by transmission electron microscopy (TEM) coupled with energy dispersive X-ray spectroscopy (EDXS) were carried out. To understand the effects of the ball milling on the pinning behavior, magnetic field and temperature dependences on a critical current density have been studied. Analyses show that Ag-milled YBCO samples exhibit higher values of critical current density in applied magnetic field compared to Ag-unmilled one. The better pinning properties of the Ag-milled samples are believed to be due to the microstructure of more fine and uniform distribution of silver and Y-deficient nanosized generated by ball milling.

Keywords YBCO superconductor · Planetary ball milling · $AgNO_3$ addition · Pinning properties

A. Hamrita · F. Ben Azzouz · W. Dachraoui · M. Ben Salem (✉)
L3M, Department of Physics, Faculty of Sciences of Bizerte, University of Carthage, 7021 Zarzouna, Tunisia
e-mail: Mohamed.bensalem@fsb.rnu.tn

1 Introduction

For most applications of high temperature superconductors (HTS), high critical current density J_c under a high magnetic field is required. Due to the granularity and porous character of HTS, polycrystalline samples exhibit low J_c value. Two main requirements must be fulfilled for producing bulk-type superconductors with a high critical current density in $YBa_2Cu_3O_7$ (Y-123 or YBCO for brevity) superconducting compound. The first is to exclude weak links in this superconductor and the second one is to introduce effective centers for pinning of magnetic flux lines. Among metallic materials, silver inclusion has a large impact on the evolution of microstructure and critical current density [1]. Artificial pinning centers can be created by various methods including chemical doping, addition of second phase particles formation of inhomogeneities, etc. [2–6]. The route of artificially introducing inhomogeneities or second-phase materials as flux pinning sites in the processing of large bulk on $YBa_2Cu_3O_7$ (Y-123 or YBCO for brevity) is a long standing topic.

Mechanical milling has been proved to be an effective technique for raising the flux pinning properties mainly in the MgB_2 compound [7–9]. For the Y-based compound, high energy ball milling has been used to produce nanocrystalline $YBa_2Cu_3O_{7-d}$ powders [10, 11]. It is reported that after about 1 h of milling, a transition from orthorhombic to tetragonal phase has been observed with total loss of superconductivity. Very recently, we have analyzed the effect of planetary mill process in YBCO compounds [12]. We reported that processing parameters of planetary ball milling technique such as ball-to-powder weight ratio, speed rotation, and number of balls have a substantial influence on the properties of the final product such as, phase homogeneity, grain size, etc. Based on these backgrounds, the ball

milling technique and Ag inclusions may be a better approach to improve critical current density and pinning properties. So, it is important to study the influence of silver addition into $YBa_2Cu_3O_{7-d}$ ceramics prepared using planetary ball milling technique and subsequent sintering at high temperature on the superconducting properties.

2 Experimental Process

Polycrystalline samples of $YBa_2Cu_3O_y$ were synthesized by solid state reaction. Details of the sample preparation have been described previously in [13], and here we give a brief description of our samples preparation. A stoichiometric mixture of Ba_2CO_3, Y_2O_3, and CuO was first calcinated in air for 12 h at 950 °C in order to produce an oxide precursor without the remainder of any carbonates. The resulting oxide precursor was subjected to two different grinding techniques, one part was milled via the planetary milling technique and another was grounded by hand in an agate mortar with an agate pestle. The precursor oxide characteristics such as size and composition are strongly affected by the impact energy input during the milling that depends on parameters of mechanical milling (e.g., ball to powder weight ratio values, high speeds of rotation, local temperature. In the present work, the ball-milling process was carried out for 4 h with a milling speed of 600 rpm and ball-to-powder weight ratio of about 5:2. The composition of the resulting milled oxide precursor is consisting of a mixture of Y-123, Y-deficient YBCO phases with additional of small quantities of superconducting phases $YBa_2Cu_4O_8$ (Y-124), $Y_2Ba_4Cu_7O_{14+x}$ (Y-247) and Y_2BaCuO_5, $BaCuO_2$ such as secondary phases. Silver was added to samples during the final processing stage. In order to mix uniformly the fine Ag particles with constituent of oxide precursor, $AgNO_3$ solution was added to the oxide precursor powder. Appropriate amounts of $AgNO_3$ solution was then mixed with the milled and hand grinding oxide precursor powders. Mixed powders were dried and then pressed uniaxially into pellets of 0.5 mm thick and 7 mm in diameter, under a pressure of 750 MPa. These pellets were sintered in air at 950 °C for 8 h and then furnace cooled to room temperature. The samples are labeled as "Ag-milled" (for planetary milled oxide precursor) and "Ag-unmilled" (for hand grinded oxide precursor).

The structure and the phase purity were examined by powder X-ray diffraction using a Scintag XDS 2000 diffractometer with CuK_α radiation. The scanning electron microscope (SEM) measurements were performed using an FEI Nano Lab 200. Chemical analysis was performed using the energy dispersive X-ray spectroscopy (EDXS) system attached to the SEM. The transport properties of the samples were studied by measuring the electrical resistivity–temperature $\rho(T)$ and current-voltage (I–V) characteristics using the four-probe technique. The pellets were carefully cut into bars shaped samples with almost similar dimensions. Electrical contacts were made using silver paint and the contact resistance value was approximately 0.5 Ω. The temperature dependence of the electrical resistivity $\rho(T)$ was measured by using the standard dc four-probe technique in a DMX-19 SCC cryostat system. The magnitude of the excitation current density, J, used to measure resistivity of the samples is $J = 40\ \mu A\,cm^{-2}$. The transport critical current density (J_{cT}) values were determined at various temperatures using a 5 μV/cm criterion and a magnetic field was applied along the short axis of the sample and the excitation current was injected along the length axis of the samples.

3 Results and Discussion

Details of the structural changes associated with the milling process and the effect of different milling parameters on the superconducting properties have already been reported elsewhere [13], and here we give a brief description of our samples characteristics. XRD analysis and SEM observations coupled with EDX analyses indicate that the milled ceramics is consisting of a mixture phases; stoichiometric YBCO and Y-deficient YBCO with a deviation of the yttrium compared to the nominal composition of $YBa_2Cu_3O_{7-\delta}$ and insignificant secondary phases such as Y-124, Y-247, Y_2BaCuO_5, and $BaCuO_2$. It is known that Y-124 and Y-247 can easily exist as an intergrowth within the Y-123 phase [14]. Y-deficient YBCO phase is presented in milled samples as nanoscale entities surrounded in the superconducting $YBa_2Cu_3O_{7-d}$ matrix. The result of resistivity versus temperature measurements indicated two resistivity drops, one starting at, $T_{c1}^{\text{onset}} = 92$ K and the other starting at $T_{c2}^{\text{onset}} \approx 90$ K. However, the unmilled sample shows a one step transition at $T_c^{\text{onset}} = 92$ K. So, the observed $T_{c2}^{\text{onset}} \approx 90$ K value is consistent with the Y-deficient YBCO phase. The zero resistance temperature, T_{co}, is 86.7 and 90 K for the milled and unmilled samples respectively. The milling process reduces the zero applied field transport critical current density J_c at 77 K; $J_c = 115\ A\,cm^{-2}$ for the milled sample, and $J_c = 160\ A\,cm^{-2}$ for the unmilled one.

XRD patterns of both milled and unmilled samples sintered with $AgNO_3$ during the final processing stage are shown in Fig. 1. Compared to nonadded samples, it should be mentioned that no noticeable difference appeared in the width and position of the diffraction peaks. Only characteristic peaks corresponding to silver have been appeared. Ag admixture seems thus to not affect the crystallographic structure of grains.

Figure 2 shows the temperature dependence of the electrical resistivity $\rho(T)$ for both milled and unmilled samples sintered with $AgNO_3$ addition. Both curves exhibit a

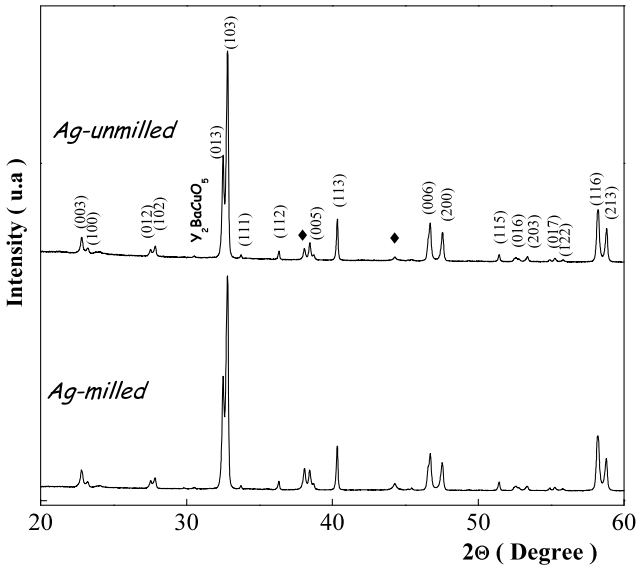

Fig. 1 X-ray powder diffraction patterns of the milled and unmilled samples sintered with $AgNO_3$ addition

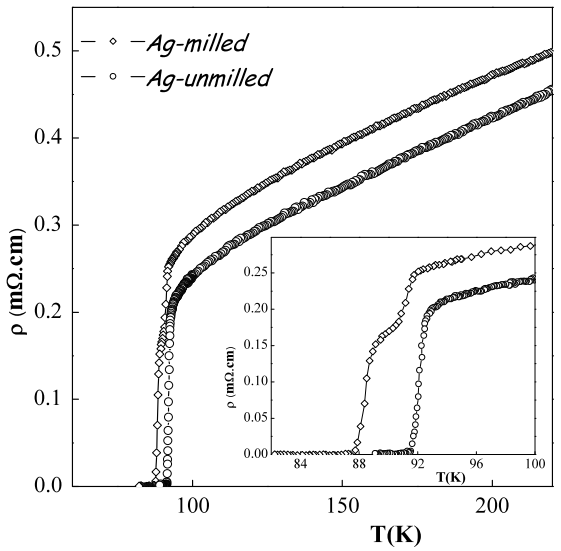

Fig. 2 Resistivity dependences on the temperature of milled and unmilled samples sintered with $AgNO_3$ addition. *Inset*: Curves of transition region for both samples

transition to the superconducting state below the onset superconducting temperature T_c^{onset} and show linear temperature dependence in the normal state. A slight increase in the zero resistance temperature T_{co} with $AgNO_3$ addition has been observed. T_{co}, is 87.4 and 90.7 K for the Ag-milled and Ag-unmilled samples, respectively. Note that the Ag-unmilled sample shows a one step transition at $T_c^{\text{onset}} = 92$ K. The result of resistivity versus temperature measurements indicated two resistivity drops one starting at $T_{c1}^{\text{onset}} = 92$ K and the other starting at $T_{c2}^{\text{onset}} \approx 90$ K. Double superconducting transitions are also observed in $Gd_{1+2x}Ba_{2+x}Cu_{3+x}O_{7-d}$ [15] in YBCO at different doping levels [16]. $AgNO_3$ addition does not affect the critical temperatures T_{c1}^{onset} and T_{c2}^{onset} in both samples. This suggests that the grains are not altered, and as a consequence the oxygen content does not change by the presence of silver. This is in excellent agreement with the XRD.

Temperature dependences of critical current density $J_c(T)$ were measured at self and applied magnetic field for samples sintered with and without $AgNO_3$ addition, and the measurements are shown in Fig. 3a and b. Two distinct behaviors can be observed from these figures. The critical current density increasing monotonically with decreasing temperature from near T_c down to $T = 20$ K for each samples. In order to understand the relevant $AgNO_3$ effect, we examined the relative change of the critical current ΔJ_c between added and free samples. Plots of ΔJ_c versus temperature are illustrated in the inset 1 of Fig. 3a.

It is clear that at a temperature less than 77 K, the $AgNO_3$ addition leads to a substantial increase of ΔJ_c values in the milled sample. The obtained J_c values are very interesting for all samples, especially when compared to the values reported in the literature in the case of polycrystalline samples added with Ag nanoparticles [17]. Generally, it is believed that Ag diffuses into the grain boundary as a metal during thermal processing and it is responsible for the increase of interconnections between the grains [18]. At a low applied magnetic field, J_c values of milled samples sintered with and without $AgNO_3$ were larger than those of free and $AgNO_3$-unmilled samples (Fig. 3b). $AgNO_3$ addition does not practically change $J_c(T)$ behavior in a low applied magnetic field. For polycrystalline HTS, the type of grain boundaries and its composition are considered as fundamental parameters that control the weak link behavior. We can estimate the electrical character (superconductor–normal–superconductor (S-N-S) or superconductor–insulator–superconductor (S-I-S) junctions) of the weak-link network in our samples using the equation $I_c = I_o(1 - T/T_{co})^{\alpha}$ for temperatures close to the superconducting transition temperature T_{co} of the intergrain junction where I_c is the critical current. The plot of $\ln(I_c)$ against $\ln(1 - T/T_{co})$ gives α as the slope value. The results are well approximated with linear fit for both samples (see inset 2 of Fig. 3) with α is about 1 which corresponds to the superconductor–insulate–superconductor (S-I-S) type joints. One can say that grain boundaries behave predominantly as SIS junctions, even in $AgNO_3$ added samples. Our results are in good agreement with ones obtained in the case of Pt doped $DyBa_2Cu_{3-x}O_y$ [19].

We have also studied the effect of an external magnetic field on the transport critical current density $J_c(H)$ at various temperatures. To isolate the flux pinning improvements, the measured $J_c(H)$ values in magnetic fields can instead be normalized to the transport critical current density at zero-field values $J_c(0)$. The dependence of the normalized critical

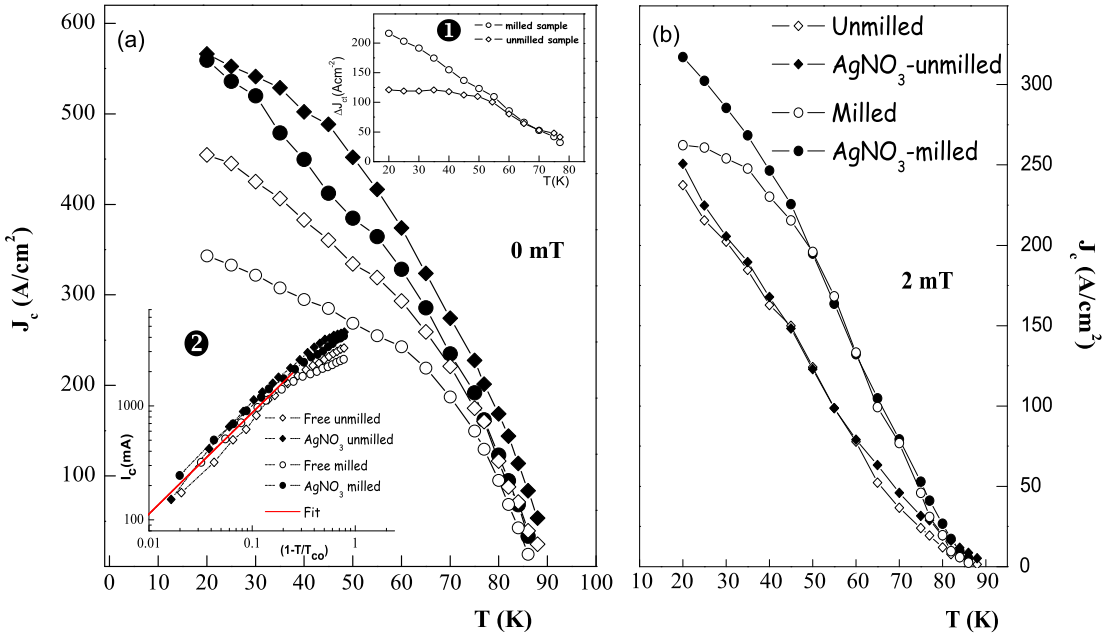

Fig. 3 Critical current density as function of temperature measured at self (**a**) and applied (**b**) magnetic field for milled and unmilled samples sintered with and without $AgNO_3$ addition. *Inset* ①: critical current density difference for both samples. *Inset* ②: critical current versus $1 - T/T_{co}$ plotted for samples on a logarithmic scale. The *solid red line* corresponds to $\alpha = 1$

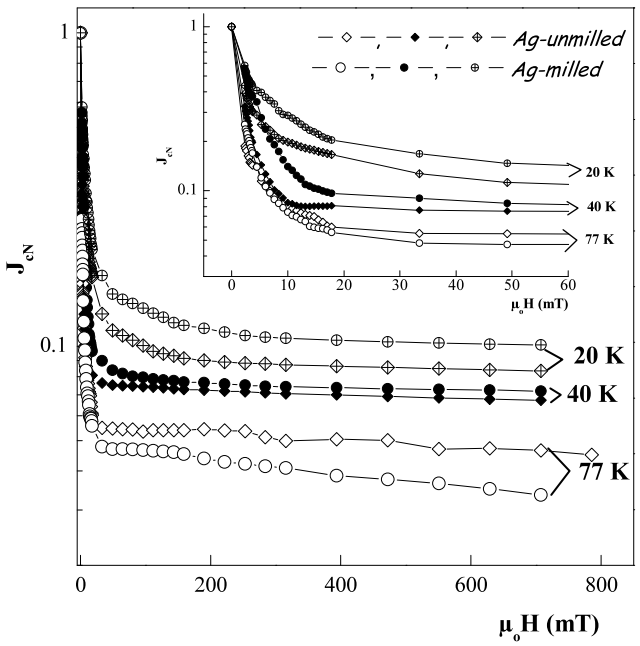

Fig. 4 Magnetic field dependence of the normalized critical current densities, J_{cN} measured at 20, 40 and 77 K for milled and unmilled samples sintered with $AgNO_3$ addition. *Inset*: J_{cN} for low applied magnetic field

current density on magnetic field, J_{cN}, $(J_{cN} = J_c(H)/J_{c0})$ in milled and unmilled samples with $AgNO_3$ additives is presented in Fig. 4. All samples show degradation of critical current density with increasing the magnetic field. At $T < 77$ K, the Ag-milled sample shows less sensitivity to magnetic field compared with Ag-unmilled sample over the entire applied magnetic fields. The $AgNO_3$-milled samples seem to have better flux pinning properties at a temperature less than 77 K. SEM micrographs of the transverse cross-section morphology of the sintered samples are shown in Figs. 5a–b. All sintered samples exhibit a granular structure with micrometer grains size. SEM micrographs of the milled sample sintered with $AgNO_3$ (Fig. 5b) exhibited entities bright in contrast with sizes ranging from 60 to 30 nm. These entities take place into the grains along with some segregation in the grain boundaries. Such entities have not been observed in unmilled samples (Fig. 5a). The EDSX resolution in the SEM observations is about 1–2 μm, so it is impractical to determine precisely the composition of entities by conducting a spot analysis on a single particle. To estimate the elemental composition of entities, comparative analyses have been carried out in the regions, where entities are present or absent. For free milled sample (see inset of Fig. 5b), the EDSX analysis performed on the area with high-density of entities clearly reveals that these entities contain Y, Ba, Cu, and O but they are consistently yttrium deficient with a deviation of the yttrium compared to the nominal composition of $YBa_2Cu_3O_y$. The chemical composition is illustrated in the inset of Fig. 5c. However, for the $AgNO_3$ milled sample, the EDSX spectrum given in the Fig. 5c shows the presence of Ag in addition to Y, Ba,

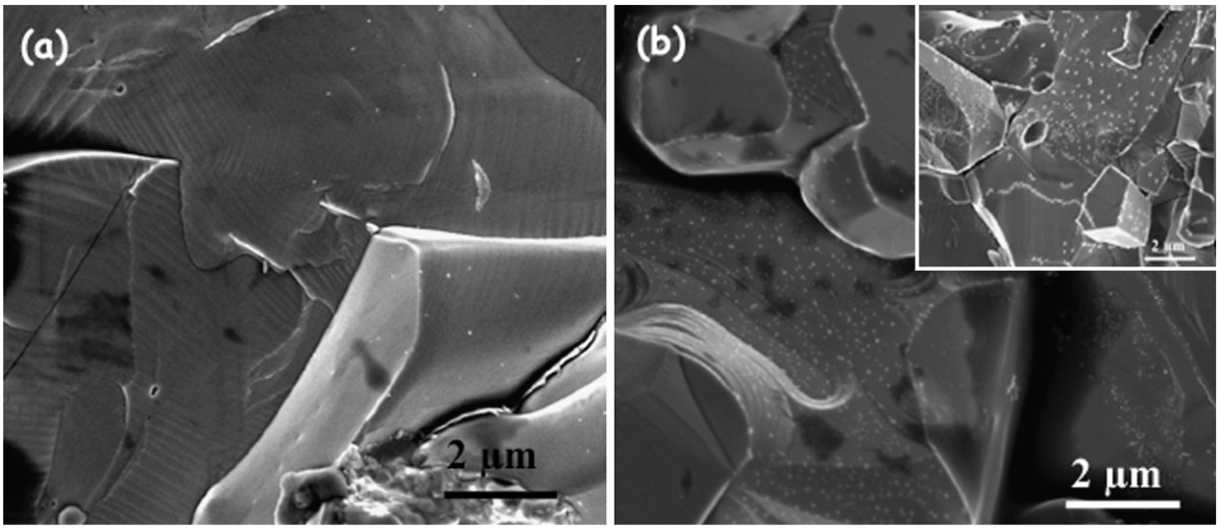

(c)

Element	atomic % measured	atomic % in stoichiometric composition
Y	7.2	16.7
Ba	36.1	33.3
Cu	55.3	50.0
Ag	1.4	0.0

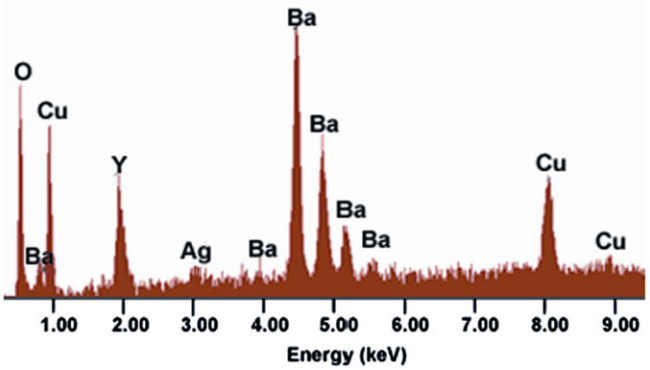

Fig. 5 SEM micrographs of (**a**) unmilled, (**b**) milled samples sintered with $AgNO_3$ additive and (**c**) EDXS spectrum taken from the area with high-density of nanoscale entities shown in (**b**). Inset of (**b**) is the SEM micrograph of free milled sample and inset of (**c**) is quantitative chemical composition

Cu, O elements. It is widely accepted that silver not reacting chemically with the YBaCuO but was shown to reside in the grain boundaries. The Ag particles are more finely and uniformly distributed at the grain boundaries of $AgNO_3$-YBCO for the milled sample than those of $AgNO_3$-YBCO of unmilled powder. For unmilled samples, Ag may be agglomerated with each other to some extent at grain boundaries after sintering and led to the formation of the stack of silver nonuniformly distributed in the sample, which reduces the effectiveness of pinning properties. Since the milled sample with the $AgNO_3$ addition revealed uniformly distributed nanosized inclusions and well dispersed of finer Ag, higher density of flux pinning sites and enhancement of critical current density can be expected at the applied magnetic field.

4 Conclusion

The effect of $AgNO_3$ additions in the microstructural evolution and related transport properties of YBCO prepared using planetary ball milling process has been investigated in comparison with the $YBa_2Cu_3O_{7-\delta}$ samples subjected to hand grinding. $YBa_2Cu_3O_{7-\delta}$ ceramics have been synthesized in air by a solid state reaction method from an oxide precursor powder, which was prepared from the starting powders of Y_2O_3, Ba_2CO_3, and CuO via a one-step annealing process in air at 950 °C. After planetary ball milling for 4 h of the oxide precursor powders, it was mixed with $AgNO_3$ solution and then was dried and uniaxially pressed, and subsequently annealed at 950 °C in air. XRD analyses indicate that silver does not react with YBCO and the milled

ceramics consists of mixture phases; stoichiometric YBCO, Y-deficient YBCO with a small deviation of the yttrium compared to the nominal composition of $YBa_2Cu_3O_{7-\delta}$ and silver phase. SEM observations coupled with EDX analyses reveal that the Y-deficient YBCO phase is presented in milled samples as nanoscale entities surround the superconducting $YBa_2Cu_3O_{7-d}$ matrix. The critical current density under applied magnetic field (J_c) of the $AgNO_3$-milled sample is higher than that of the Ag-unmilled one. The better pinning properties of the Ag-milled samples are believed to be due to the microstructure of more finely and uniformly distributed of silver and Y-deficient nanosized generated by ball milling.

References

1. Tepea, M., Avcia, I., Kocoglua, H., Abukayb, D.: Solid State Communications **131**, 319 (2004)
2. Larbalestier, D., Gurevich, A., Feldmann, D.M., Polyanski, A.: Nature **414**, 368 (2001)
3. Goswami, R., Haugan, T.J., Barnes, P.N., Spanos, G., Holtz, R.L.: Physica C **470**, 318 (2010)
4. Ben Azzouz, F., Zouaoui, M., Mellekh, A., Annabi, M., Van Tendeloo, G., Ben Salem, M.: Physica C **455**, 25 (2007)
5. Zhao, Y., Cheng, C.H., Wang, J.S.: Supercond. Sci. Technol. **18**, S43 (2005)
6. Liyanawaduge, N.P., Kumar, A., Kumar, S., Karunarathne, B.S.B., Awana, V.P.S.: J Supercond Nov Magn **25**, 31 (2012)
7. Strickland, N.M., Buckley, R.G., Otto, A.: Appl. Phys. Lett. **83**, 326 (2003)
8. Lee, J.H., Shin, S.Y., Kim, C.J., Park, H.W.: J. Alloys Compd. **476**, 919 (2009)
9. Xu, X., Kim J, H., Duo, S.X.: J. Appl. Phys. **105**, 103913 (2009)
10. Simoneau, M., L'Espérance, G., Trudeau, M.L., Schulz, R.: Mater Res J. **9**, 535 (1994)
11. Xiang, J.Y., Fleck, C., Hampshire, D.P.: Journal of Physics: Conference Series **97**, 012237 (2008)
12. Hamrita, A., Ben Azzouz, F., Madani, A., Ben Salem, M.: Physica C **472**, 34 (2012)
13. Hamrita, A., Ben Azzouz, F., Dachraoui, W., Ben Salem, M.: submitted to Physica C
14. Van Tendeloo, G., Brodin, D., Zandbergen, H.W., Amelinckx, S.: Physcia C **167**, 627 (1990)
15. Zhang, H., Liu, Y., Li, H.L., Qu, J.F., Li, X.G., Feng, Y.: Supercond. Sci. Technol. **18**, 1317 (2005)
16. Lortz, R., Tomita, T., Wang, Y., Junod, A., Schilling, J.S., Masui, T., Tajima, S.: Physica C **434**, 194 (2006)
17. Farbod, M., Reza Batvandi, M.: Physica C **471**, 112 (2011)
18. Zhao, Y., Cheng, C.H.: Physica C **386**, 286 (2003)
19. Orlova, T.S., Laval, J.Y., Nguyen-van-Huong, C., Dubon, A.: Supercond. Sci. Technol. **1156**, 12 (1999)